Atmos. Chem. Phys. Discuss., 7, 17741–17767, 2007
www.atmos-chem-phys-discuss.net/7/17741/2007/

Atmospheric Chemistry and Physics Discussions

Measurement of the water vapour vertical profile and of the Earth's outgoing far infrared flux

L. Palchetti, G. Bianchini, B. Carli, U. Cortesi, and S. Del Bianco

Istituto di Fisica Applicata "Nello Carrara" – Consiglio Nazionale delle Ricerche IFAC–CNR, Sesto Fiorentino, Firenze, 50019, Italy

Received: 18 October 2007 – Accepted: 26 November 2007 – Published: 10 December 2007

Correspondence to: L. Palchetti (l.palchetti@ifac.cnr.it)

Abstract

Our understanding of global warming depends on the accuracy with which the atmospheric components that modulate the Earth's radiation budget are known. Many uncertainties still exist on the radiative effect of water in the different spectral regions, among which the far infrared where few observations have been made. An assessment is shown of the atmospheric outgoing flux obtained from a balloon-borne platform with wideband spectrally resolved nadir measurements at the top-of-atmosphere over the full spectral range, including the far infrared, from 100 to 1400 cm^{-1}, made by a Fourier transform spectrometer with uncooled detectors. From these measurements, we retrieve 15 pieces of information about water vapour and temperature profiles, and surface temperature, with a precision of 5% for the mean water vapour profile and a major improvement of the upper troposphere-lower stratosphere knowledge. The retrieved atmospheric state makes it possible to calculate the emitted radiance as a function of the zenith angle and to determine the outgoing radiation flux, proving that spectrally resolved observations can be used to derive accurate information on the integrated flux. While the retrieved temperature is in good agreement with ECMWF analysis, the retrieved water vapour profile differs significantly, and, depending on time and location, the derived flux differs in the far infrared (0–600 cm^{-1}) from that derived from ECMWF by 2–3.5 $W/m^2 \pm 0.4$ W/m^2. The observed discrepancy is larger than current estimates of radiative forcing due to CO_2 increases since pre-industrial time. The error with which the flux is determined is caused mainly by calibration uncertainties while detector noise has a negligible effect, proving that uncooled detectors are adequate for top of the atmosphere radiometry.

1 Introduction

Water is the principal molecule driving the climate on Earth since through the hydrologic cycle it is involved in all the phenomena from energy transport to radiative effects gov-

ACPD

7, 17741–17767, 2007

erning the climate system (Pierrehumbert, 2002). The atmospheric water, in the form of both vapour and clouds, is the most important greenhouse components trapping the outgoing longwave radiation (OLR) (Harries, 1996). Even if its main contribution to climate changes is through feedback processes occurring as a consequence of a man-induced temperature variation driven by the increased CO_2 concentration, it has recently been found that also long term increases in stratospheric water vapour may be considered to be in part a forcing term (Held and Soden, 2000). Changes in the distribution of water vapour and the associated radiative forcing and feedback are well recognised as fundamental processes to be characterised in predicting future climate (Lindzen, 1990; Chahine, 1992; Harries, 1997; Stuber et al., 2005). 2007 IPCC report identifies the estimate of the strength of different feedbacks as a key uncertainty in global circulation model predictions (Randall et al., 2007).

Despite its prominent spectroscopic signatures in the OLR, the quantitative measurement of the water vapour volume mixing ratio (VMR) is made difficult by its variability and its large vertical (and to a lesser extent horizontal) concentration gradients. Furthermore, also the spectroscopy of water vapour poses some problems. The high concentration of this species in the lower troposphere makes relevant several spectroscopic processes (self and foreign broadening, pressure shift, and continuum absorption) (Tobin et al., 1999) that are difficult to observe in laboratory conditions and require a field validation. In this context, Sinha and Harries (1995) pointed out the lack of validation of far infrared (FIR) model line parameters of water vapour under atmospheric conditions and stressed that FIR parameterisation in climate models should be validated by observational programs.

The radiative balance of the troposphere is influenced strongly by radiative cooling associated with the emission of FIR radiation by water vapour. The water vapour rotational band is extremely intense, especially at band centre around 200–300 cm^{-1}, and so emits to space from the upper troposphere. Atmospheric fluxes calculations (Clough et al., 1992) have shown that perturbations to upper tropospheric water vapour (pressures of <500 hPa) exert a peak response in the FIR, and can have a sizeable im-

ACPD
7, 17741–17767, 2007

pact on the clear-sky greenhouse effect.

Water can manifest itself also in the form of cirrus clouds and cirrus cloud feedback is the major source of discrepancy between models of climate predictions. The prevalence and persistence of cirrus cloud systems, especially in the tropical upper troposphere, implies that cirrus clouds play an important role in climate (Liou, 1986). Radiative studies of cirrus clouds show that the clouds may cool radiatively or heat the upper atmosphere in the thermal infrared wavelengths depending upon height, thickness and microphysics of the particles (Cox, 1971; Stephens et al., 1990). Cirrus clouds have been recognised as important components of feedback processes to climate forcings (Randall et al., 1989; Del Genio et al., 1996; Chou and Neelin, 1999). The OLR flux is strongly modulated by cirrus, nevertheless, the available operative sensors give no direct information on cloud microphysics and cirrus clouds represent a major observational gap.

In this contest, in June 2005 we performed a new spectral measurement, described in Sect. 2, covering the FIR portion of the Earth's emission spectrum, from a stratospheric balloon flown in tropical region in the North-East of Brazil. As described in Sect. 3, this spectral measurement allows the retrieval of temperature and water vapour vertical profiles up to the upper troposphere level. A comparison of our results with the atmospheric status obtained from the ECMWF (European Centre for Medium-range Weather Forecast) analysis is shown in Sect. 4. In Sect. 5 the difference from ECMWF found on the water vapour concentration profile is used to address the effect on the calculation of the outgoing longwave radiation flux at the flight altitude level.

2 Spectroscopic measurements of the outgoing longwave radiation

In June 2005 the first wideband spectrally resolved measurements including the FIR portion of the atmospheric thermal emission were performed from stratospheric balloon platform. Two experiments were flying almost at the same time, the FIRST (Far InfraRed Spectroscopy of the Troposphere) experiment flew from Fort Sumner

(NM, USA) on 7 June, and the REFIR-PAD (Radiation Explorer in the Far InfraRed-Prototype for Applications and Development) experiment flew from Teresina (Brazil) on 30 June. FIRST measurements were performed with a broad bandpass Fourier transform spectrometer (FTS) with Michelson configuration, covering the 50–2000 cm^{-1} spectral range, with 0.625 cm^{-1} resolution. The instrument is partially cooled: aft optics at 180 K, and detectors at 4.2 K. REFIR-PAD measurements were performed with a FTS with Mach-Zehnder configuration covering the 100–1400 cm^{-1} spectral range with 0.5 cm^{-1} resolution.

REFIR-PAD is a prototype developed as a field demonstrator of a satellite instrument designed in the framework of the European REFIR space mission (European-Commission, 2000; Rizzi et al., 2002). It is a compact and innovative FTS with double-input/double-output port configuration designed for measuring with high accuracy the wideband atmospheric emission without requiring any cooled components (Palchetti et al., 2005; Bianchini et al., 2006). This instrument is optimised as a small and light payload and uses uncooled optics and detectors. The capability of an uncooled instrument to provide information on the status of the atmosphere and its radiative properties is assessed in the present paper.

REFIR-PAD acquired 540 nadir spectra of the atmospheric emission during a stratospheric flight at the mean floating altitude of 34 km for about 8 h (Palchetti et al., 2006). The experiment was launched onboard a gondola that hosted the LPMAA IASI–balloon (Laboratoire de Physique Moléculaire pour l'Atmosphère et l'Astrophysique – Infrared Atmospheric Sounding Interferometer) instrument from the airfield of Timon, near Teresina in the North-East Brazil (5°5′ S, 42°52′ W), at night at 03:36 local time, and landed 10 h later at 270 km south-west of the launch site. This tropical flight was performed within the framework of the Equatorial Large Balloons Campaign (ELBC) led by the French Centre National d'Etudes Spatiales (CNES) in collaboration with the European Space Agency (ESA), for the Envisat (Environmental Satellite) validation program.

A summary of the main instrument specifications including performances for this

ACPD
7, 17741–17767, 2007

flight is reported in Table 1. An accurate characterisation of the level 1 analysis producing calibrated spectra can be found in Bianchini and Palchetti (2007). The noise equivalent spectral radiance (NESR) turned out to be in the range of 0.8–2.5 mW/(m^2 sr cm^{-1}) with the lower values between 200 and 600 cm^{-1}. The mean calibration error was about 0.1 K with a peak-to-peak value of about ±0.3 K. The total radiometric error has been calculated as a function of frequency for each calibrated spectrum taking into account both the detector noise component and the systematic calibration errors.

3 Retrieval of water vapour and temperature vertical profiles

Nadir wideband spectral measurements have been used to retrieve the vertical profiles of atmospheric temperature and water vapour concentration, and the surface (skin) brightness temperature (BT). Vertical profile of temperature is retrieved exploiting the carbon dioxide band at 668 cm^{-1}. A trend corrected value of carbon dioxide of 378 ppmv is considered. The water vapour profile is retrieved exploiting both the vibro-rotational band and the FIR pure rotational band below 600 cm^{-1}. The software devoted to the analysis of REFIR-PAD measurements has been developed at IFAC. The main features of the retrieval code can be described by making reference to two main blocks: the forward model and the inverse model.

3.1 Forward model

The forward model simulates REFIR-PAD wideband measurements using line-by-line radiative transfer (RT) calculation. The code computes the radiance that reaches the instrument, and simulates the instrumental effects (instrumental lineshape and field of view). Assuming a uniform layered atmosphere, the RT has been implemented using the Curtis-Godson (Houghton, 2002) values associating a temperature and pressure equivalent value to each species in the layer in order to evaluate the averaged value of the cross-section. The atmospheric lineshapes are modelled with a modified

ACPD
7, 17741–17767, 2007

Voigt profile in which the Lorentz function is replaced with the Van Vleck-Weisskopf (Van Vleck and Weisskopf, 1945) function. The spectroscopic database used for the simulations is HITRAN 2004 (Rothman et al., 2005) with recent updates for the air broadened half widths provided by Gordon et al. (2007). The atmospheric continuum is modelled according to the work by Clough et al. (2005) considering the contribution of water vapour lines external to the region of $\pm 25\,cm^{-1}$ from the line centre. For CO_2 a dedicated database and lineshape has been adopted in order to take into account the line-mixing effect (Niro et al., 2005a,b).

3.2 Inversion

The retrieval procedure (Carli et al., 2007) uses the constrained Non-linear Least-Square Fit (NLSF) approach: the cost function to be minimised takes into account the a priori information (optimal estimation approach) and the Marquardt lambda parameter (Rodgers, 2000). The retrieval algorithm enables us to fit the wideband spectrum to find more quantities simultaneously (multi-target retrieval) in order to best account for the errors due to the interfering unknowns.

REFIR-PAD measurements have been analysed by simultaneously fitting the water vapour profile, the temperature profile and the Earth skin BT using the spectrum from 100 to $1000\,cm^{-1}$. As a priori information, the IG2 database (Remedios, 1999) for an equatorial atmosphere in July 2005 has been used. The pressure profile at the altitude grid provided by ECMWF database has been obtained by imposing the hydrostatic equilibrium with a pressure reference level at 1000 hPa. The a priori errors that have been used are 100% for water vapour profile and a linearly decreasing error from 9.8 K at an altitude of 1 km to 2.3 K at an altitude of 33 km for the temperature profile. The convergence is established using the chi-square test. The final reduced chi-square close to one indicates the agreement between the forward model and measurements and the correctness of the estimated measurement noise. The correlations among the products are contained in the correlation matrix exported by the program.

In Fig. 1 and Fig. 2 an example of the retrieved profiles from the output provided by

the analysis is given. The plots show the retrieved profiles (red lines) with the constrained error together with the initial guess profile (blue lines) and the profile obtained from the ECMWF operational analysis (green lines). The results show a good agreement with ECMWF for the temperature profile and for water vapour below 10 km altitude. Above 10 km, REFIR-PAD measurement found a drier atmosphere which alters the result of the calculation of the OLR flux, as it will shown in Sect. 5.

The retrieval altitude grid has been optimised in order to maximise the total number of independent retrieved unknowns and to better exploit the sounding capability of the REFIR-PAD instrument. The analysis of the averaging kernel profiles for temperature and water vapour VMR, shown in Fig. 3 and Fig. 4 respectively, was used to select the vertical retrieval grid. The results shows that REFIR-PAD measurements provide information up to 33 km for temperature, and up to about 17 km for water vapour, with a vertical resolution of about 2 km for both quantities.

The degrees of freedom of the retrieval, i.e. the number of independent new pieces of information provided by the trace values of the averaging kernel matrix, are for atmospheric temperature, water vapour, and surface skin BT, 7, 7, and 1, respectively. The information content coming from the FIR region improves the water vapour retrieval in the upper troposphere relative to retrievals only performed in the rotovibrational band (Mertens, 2002).

3.3 Error budget

The error analysis takes into account both the random measurement noise (NESR) due to the detector and the spectrally-correlated calibration uncertainty. In the case of the REFIR-PAD measurement, the NESR is due to the uncooled pyroelectric detectors and, as we have seen in Sect. 2, it is in the range of 0.8–2.5 mW/(m^2 sr cm^{-1}). Also the measurement noise of the calibration spectra contributes to this error, which has no correlation among the different spectral channels. The second effect is instead calculated with 1σ-error corresponding to the peak error of 0.3 K in the knowledge of the calibration sources temperature and it is less than 1.2 mW/(m^2 sr cm^{-1}). This error

ACPD
7, 17741–17767, 2007

is correlated among the different spectral channels. An in-deep analysis of these errors and of their spectral features can be found in Bianchini and Palchetti (2007).

A full variance-covariance matrix of these errors is used to assess the error propagation in the retrieved atmospheric state. In such a way, an error of about 2 K constant at different altitudes is found for the temperature profile, and an error varying from 22% at ground to 35% at 17 km altitude for water vapour. These errors are shown by error bars in Figs. 1 and 2. The skin BT is retrieved with an errore of about 0.4 K.

4 Data analysis: atmospheric state

Some thin scattered clouds were present at low altitude at the beginning of the flight, but apart a small effect observed soon after launch, the atmosphere resulted to be transparent enough to assume clear sky in our analysis. The vertical profiles of water vapour VMR and temperature, and the skin BT have been retrieved for each measurement sequence during the flight from 08:05 to 15:47 UTC. A mean spectrum is obtained for each sequence by a weighted average of 10 spectra acquired in about 6 min.

In order to check the validity of the vertical profiles of temperature and water vapour retrieved from REFIR-PAD measurements, we relied on correlative data obtained from ECMWF operational analysis. Vertical profiles of temperature and relative humidity (converted to water vapour VMR) for the region of Teresina, Brazil and for the duration of the balloon flight were obtained from the ECMWF data archive, with a spatial resolution of $1^{\circ}\times1^{\circ}$ in latitude and longitude and with a temporal resolution of 6 h. These profiles were linearly interpolated to the average geolocation and time of each REFIR-PAD sequence. The resulting temperature and water vapour distributions were used for validation purposes.

The REFIR-PAD profiles retrieved during the flight were compared with the ECMWF correlative data. The comparisons are shown in Fig. 5 for the temperature profiles and in Fig. 6 for the water vapour profiles. The differences for temperature are generally low and in particularly they seldom exceed 2%. For the water vapour VMR, instead Fig. 6

ACPD
7, 17741–17767, 2007

shows that the retrieved profiles are characterised by a drier upper troposphere, about 60% less that the ECMWF VMR in in the region from 12 km to tropopause. The greater differences observed at lower altitudes at the beginning of the flight are possibly due to a pixel contamination produced by the presence of clouds.

In Fig. 7, we report the mean values of the residuals of the fitting process, obtained by averaging over the duration of the flight the difference between the observed spectral radiance and its simulated values after last iteration (red line). The average of the residuals is compared with the mean value over the flight of the measurement error, computed as the root mean square of the diagonal elements of the variance-covariance matrix of the observations. The residuals are generally well within the mean measurement error, with isolated exceptions that peak around 460 cm^{-1} and 590 cm^{-1}, proving that no significant unaccounted systematic error is present in the data analysis (Bianchini et al., 2007).

In Fig. 8, the time series of the temperature values at the retrieval altitudes are displayed for the lower troposphere. The ground skin BT increment due to the solar irradiation was detected starting from the sunrise occuring at sequence #19. A small increment of temperature is also observed in the first layer of the atmosphere.

Since the atmospheric state is sufficiently uniform in time and location along the flight, the retrieval standard error, described in Sect. 3.3, can be compared with the standard deviation of all the measurements. The comparison shows a good agreement between the two sets of values for both temperature and water vapour. This allows to consider the mean standard error of the mean measurement, which resulted to be less than 0.5 K for temperature mean profile, and about 3–5% for water vapour mean profile.

5 Data analysis: outgoing longwave radiation flux

The evaluation of the OLR by using directional non-spectral measurements, such as satellite single view observations, is affected by an error due to the angular distribution model used for the calculation of the emission anisotropy factor

in the radiance-to-flux conversion, see e.g. the ERBE and CERES experiments (Suttles et al., 1992; Wielicki et al., 1996). It was shown that statistical methods developed for deriving the anisotropy factor for different viewing conditions are affected by an error of about 4.6 W/m^2 for the best situation of nadir observations (Clerbaux et al., 2003).

Our spectrally resolved measurement provides the capability of retrieving the atmospheric parameters, that primarily determine the OLR emission, i.e. the vertical profiles of T and water vapour, and the surface emission. Based on this information and using a RT model, such as that described in Sect. 3.1, it is possible to simulate the emission $L(\sigma,\theta)$ as a function of the wavenumber σ and the zenith angle θ. In the case of an horizontally uniform atmosphere, the angular integral defining the OLR flux F_{OLR} is accurately calculated with the following equation

$$F_{\mathrm{OLR}} = 2\pi \int_0^{\infty} d\sigma \int_0^{\frac{\pi}{2}} L(\sigma,\theta)\cos(\theta)\sin(\theta)d\theta. \quad (1)$$

and has a variance equal to:

$$\sigma^2_{F_{\mathrm{OLR}}} = 4\pi^2 \int_0^{\infty} d\sigma_1 \int_0^{\infty} d\sigma_2 \int_0^{\frac{\pi}{2}} d\theta_1 \cos(\theta_1)\sin(\theta_1) \cdot \cdot \int_0^{\frac{\pi}{2}} d\theta_2 \cos(\theta_2)\sin(\theta_2)\mathbf{J}_1\mathbf{S}\mathbf{J}_2^T. \quad (2)$$

where $\mathbf{S}$ is the variance covariance matrix of the retrieved atmospheric parameters, $\mathbf{J}_1$ and $\mathbf{J}_2$ are the jacobian matrices

$$(\mathbf{J}_k)_{\sigma_i,j} = \frac{\partial L(\sigma_i,\theta_k)}{\partial x_j}. \quad (3)$$

where x_i are the retrieved parameters.

Equation (1) was used with our measurements for the calculation of F_{OLR} at the floating altitude of the balloon gondola. The integral is calculated with a spectral integration from 20 to 2600 cm^{-1} and with the simulation of different angular observations from the zenith to the atmospheric limb. The limitation in the spectral domain introduces an underestimation of about 0.05 W/m^2 in our case of the tropical atmosphere. The OLR flux varies along the flight path mainly due to the temperature variations of the lower troposphere and of the Earth surface. The value has the minimum of 284 W/m^2 at the sunrise occurring at 09:00 UTC and reaches 306 W/m^2 at the end of the flight at 15:48 UTC. The error analysis shows that the effect of random noise on the flux integral is negligible since it has positive and negative contributions which cancel out along the wavenumber integration performed to calculate the flux. The systematic component due to the calibration accuracy is instead integrated with the flux and is the main contribution to the total error. With this analysis, we found that the radiation flux error is about 0.4 W/m^2 when related to the FIR spectral region and globally over the whole band it does not exceed 1.3 W/m^2.

A comparison with the fluxes calculated for the ECMWF atmospheric states has been performed in the two extreme cases at sunrise and at the end of flight. Also the fluxes obtained with the ECMWF atmosphere show an increase with time, but both the ECMWF fluxes and their increase are less that what obtained with REFIR-PAD data. The FIR spectral region from 0 to 600 cm^{-1} is here considered in detail because in this spectral region new observations are obtained by REFIR-PAD and low altitude clouds have a negligible effect on the TOA radiance. The result is shown in Fig. 9, where in the top panel the differences between the spectral fluxes calculated for the retrieved and the ECMWF water vapour and temperature profiles are shown for the sunrise (blue line), and for the end of the flight (red line). In the bottom panel, the results are reported as the cumulative integral of the spectral differences and they are compared with the cumulative integral of the expected error (dashed lines). The Fig. 9 shows that the OLR flux differences in the FIR are in the range of 2–3.5 W/m^2, larger for the warmer atmosphere.

ACPD
7, 17741–17767, 2007

This result clearly identifies the differences with the estimations made with the ECMWF atmospheric analysis and the importance of the characterisation of the FIR region for the exact calculation of the OLR fluxes. The error with which the flux is determined is caused mainly by calibration uncertainties while detector noise has a negligible effect. This is a further demonstration that uncooled detectors are adequate for a detailed radiometric observations.

6 Conclusions

The results of the first flight of REFIR-PAD have been shown. The instrument performed the spectral measurement of the OLR from 100 to 1400 cm^{-1} in the tropical region in June 2005. This spectrally resolved measurement has allowed the retrieval of the atmospheric state with sufficient precision to improve the accuracy with which the integrated outgoing radiation flux can be calculated, proving that spectral information can be used to infer the angular distribution of the radiance.

While the temperature profile is in good agreement with the ECMWF analysis, the retrieved water vapour VMR profile differs of about 60% at the upper troposphere – lower-stratosphere altitude. This difference allows to calculate the difference in terms of the OLR flux at the flight altitude of 34 km due to the FIR region which resulted to be as large as 3.5 W/m^2 with an error of about 0.4 W/m^2. A difference of 3.5 W/m^2 is an important term in the determination of the total OLR since it is comparable to or even greater than the estimation of the radiative forcing of the CO_2 increases since pre-industrial times.

Furthermore, we have shown that the flux error is mainly due to the radiometric calibration uncertainty while the random detector noise has a negligible effect, proving the feasibility of climatological studies with instruments that use uncooled detectors.

This measurement that is limited in time and space can not be representative of a bias in ECMWF analysis, but underlines a shortcoming in the knowledge of the Earth's radiation budget. We argue that a comprehensive characterisation of the outgoing ra-

diation flux could be attained, using uncooled detectors, from spectrally resolved wide-band measurements of the atmospheric emission, that also includes the far infrared.

Acknowledgements. The Authors wish to thank C. Camy-Peyret, LPMAA-CNRS, France, the CNES ballon team (led by P. Chadoutaud), and the CNES gondola team (led by J. Evrard) for having hosted REFIR-PAD on-board the IASI-balloon gondola and the helpful support during the Brazilian field campaign.

References

Bianchini, G. and Palchetti, L.: REFIR-PAD level 1 data analysis and performance characterization, Atmos. Chem. Phys. Discuss., accepted, 2007. 17746, 17749

Bianchini, G., Palchetti, L., and Carli, B.: A wide-band nadir-sounding spectroradiometer for the characterization of the Earth's outgoing long-wave radiation, 6361, p.63 610A, 2006. 17745

Bianchini, G., Carli, B., Cortesi, U., Bianco, S. D., Gai, M., and Palchetti, L.: Test of far infrared atmospheric spectroscopy using wide band ballon borne measurements of the upwelling radiance, J. Quant. Spectrosc. Rad., doi:10.1016/j.jqsrt.2007.11.010, 2007. 17750

Carli, B., Bazzini, G., Castelli, E., Cecchi-Pestellini, C., Bianco, S. D., Dinelli, B. M., Gai, M., Magnani, L., Ridolfi, M., and Santurri, L.: MARC: A code for the retrieval of atmospheric parameters from millimeter-wave limb measurements, J. Quant. Spectrosc. Rad., 105, 476–491, 2007. 17747

Chahine, M.: The hydrological cycle and its influence on climate, Nature, 359, 373–380, 1992. 17743

Chou, C. and Neelin, J.: Cirrus Detrainment-Temperature Feedback, Geophys. Res. Lett., 26, 1295–1298, 1999. 17744

Clerbaux, N., Dewitte, S., Gonzalez, L., Bertrand, C., Nicula, B., and Ipe, A.: Outgoing long-wave flux estimation: improvement of angular modelling using spectral information, Remote Sens. Environ., 85, 389–395, 2003. 17751

Clough, S. A., Iacono, M. J., and Moncet, J.-L.: Line-by-Line Calculations of Atmospheric Fluxes and Cooling Rates: Application to Water Vapor, J. Geophys. Res., 97, 15 761–15 785, 1992. 17743

Clough, S. A., Shepard, M. W., Mlawer, E. J., Delamere, J. S., Iacono, M. J., Cady-Pereira, K.,

Boukabara, S., and Brown, P. D.: Atmospheric radiative transfer modelling: a summary of the AER codes, J. Quant. Spectrosc. Rad., 91, 233–244, 2005. 17747
Cox, S.: Cirrus Clouds and the Climate, J. Atmos. Sci., 28, 1513–1515, 1971. 17744
European-Commission: REFIR Radiation Explorer in the Far InfraRed, Tech. Rep. Final ENV4-CT6-0344, European Commission, Brussels, Belgium, 2000. 17745
Del Genio, A. D., Yao, M.-S., Kovari, W., , and Lo, K. K.-W.: A prognostic cloud water parameterization for global climate models, J. Climate, 9, 270–304, 1996. 17744
Gordon, I. E., Rothman, L. S., Gamache, R. R., Jacquemart, D., Boone, C., Bernath, P. F., Shephard, M. W., Delamere, J. S., and Clough, S. A.: Current updates of the water-vapor line list in HITRAN:A new "Diet" for air-broadened half-widths, J. Quant. Spectrosc. Rad., 108, 389–402, 2007. 17747
Harries, J. E.: Atmospheric radiation and atmospheric humidity, Q. J. Roy. Meteor. Soc., 123, 2173–2186, 1997. 17743
Harries, J. E.: The Greenhouse Earth – A view from space, Q. J. Roy. Meteor. Soc., 122, 799–818, 1996. 17743
Held, I. M. and Soden, B. J.: Water vapor feedback and global warming, Annu. Rev. Energ. Env., 25, 441–475, 2000. 17743
Houghton, J.: The physics of atmospheres, Cambridge University Press, Cambridge, U.K., New York, 2002. 17746
Lindzen, R.: Some Coolness Concerning Global Warming, Bull. Amer. Meteor. Soc., 71, 288–299, 1990. 17743
Liou, K.-N.: Influence of cirrus clouds on weather and climate processes, a global perspective, Mon. Weath. Rev., 114, 1167–1199, 1986. 17744
Mertens, C. J.: Feasibility of retrieving upper tropospheric water vapor from observations of far-infrared radiation, 4485, pp.191–201, SPIE, 2002. 17748
Niro, F., Jucks, K., and Hartmann, J. M.: Spectra calculations in central and wing regions of CO_2 IR bands. IV: software and database for the computation of atmospheric spectra, J. Quant. Spectrosc. Rad., 95, 469–481, 2005a. 17747
Niro, F., Von Clarmann, T., Jucks, K., and Hartmann, J. M.: Spectra calculations in central and wing regions of CO_2 IR bands between 10 and 20 μm. III: atmospheric emission spectra, J. Quant. Spectrosc. Rad., 90, 61–76, 2005b. 17747
Palchetti, L., Bianchini, G., Castagnoli, F., Carli, B., Serio, C., Esposito, F., Cuomo, V., Rizzi, R., and Maestri, T.: The breadboard of the Fourier transform spectrometer for the Radiation

Explorer in the Far Infrared (REFIR) atmospheric mission, Appl. Opt., 44, 2870–2878, 2005. 17745
Palchetti, L., Belotti, C., Bianchini, G., Castagnoli, F., Carli, B., Cortesi, U., Pellegrini, M., Camy-Peyret, C., Jeseck, P., , and Té, Y.: Technical note: First spectral measurement of the Earth's upwelling emission using an uncooled wideband Fourier transform spectrometer, Atmos. Chem. Phys., 6, 5025–5030, 2006. 17745
Pierrehumbert, R.: The hydrologic cycle in deep-time climate problems, Nature, 419, 191–198, 2002. 17743
Randall, D., Wood, R., and et al.: Climate Models and Their Evaluation, chap. 8, IPCC WG1 AR4 Final Report, 2007. 17743
Randall, D. A., Harshvardhan, Dazlich, D. A., and Corsetti, T. G.: Interactions among Radiation, Convection, and Large-Scale Dynamics in a General Circulation Model, J. Atmos. Sci., 47, 1943–1970, 1989. 17744
Remedios, J. J.: Extreme atmospheric constituent profiles for MIPAS, 2, pp. 779–783, 96, 1999. 17747
Rizzi, R., Palchetti, L., Carli, B., Bonsignori, R., Harries, J. E., Leotin, J., Peskett, S. C., Serio, C., and Sutera, A.: Feasibility of the spaceborne radiation explorer in the far infrared (REFIR), 4485, pp. 202–209, SPIE, http://link.aip.org/link/?PSI/4485/202/1, 2002. 17745
Rodgers, C. D.: Inverse Methods for Atmospheric Sounding: Theory and Practice, World Scientific, Singapore, New Jersey, London, Hong Kong, 2000. 17747
Rothman, L. S., Jacquemart, D., Barbe, A., Benner, D. C., Birk, M., Brown, L. R., Carleer, M. R., and Wagner, .G.: The HITRAN 2004 molecular spectroscopic database, J. Quant. Spectrosc. Rad., 96, 139–204, 2005. 17747
Sinha, A. and Harries, J. E.: Water vapor and greenhouse trapping: the role of far infrared absorption, Geophys. Res. Lett., 22, 2147–2150, 1995. 17743
Stephens, G., Tsay, S., Stackhouse, P. J., and Flatau, P.: The Relevance of the Microphysical and Radiative Properties of Cirrus Clouds to Climate and Climatic Feedback, J. Atmos. Sci., 47, 1742–1754, 1990. 17744
Stuber, N., Ponater, M., and Sausen, R.: Why radiative forcing might fail as a predictor of climate change, Clim. Dynam., 2005. 17743
Suttles, J. T., Wielicki, B. A., and Vemury, S.: Top-of-Atmosphere Radiative Fluxes: Validation of ERBE Scanner Inversion Algorithm Using Nimbus-7 ERB Data, J. Appl. Meteor., 31, 784–796, 1992. 17751

Tobin, D. C., Best, F. A., Brown, P. D., Clough, S. A., Dedecker, R. G., Ellingson, R. G., Garcia, R. K., Howell, H. B., Knuteson, R. O., Mlawer, E. J., Revercomb, H. E., Short, J. F., van Delst, P. F. W., and Walden, V. P.: Downwelling spectral radiance observations at the SHEBA ice station: Water vapor continuum measurements from 17 to 26 μm, J. Geophys. Res., 104, 2081–2092, 1999. 17743

Van Vleck, J. H. and Weisskopf, V. F.: On the Shape of Collision-Broadened Lines, Revs. Mod. Phys., 17, 227–236, 1945. 17747

Wielicki, B. A., Barkstrom, B. R., Harrison, E. F., Lee, R. B., Louis Smith, G., and Cooper, J. E.: Clouds and the Earth's Radiant Energy System (CERES): An Earth Observing System Experiment, Bull. Amer. Meteor. Soc., 77, 853–868, 1996. 17751

Table 1. REFIR-PAD specifications.

Spectrometer specifications	
Interferometer type	Mach-Zehnder with double-input/double-output
Detector system	2 room temperature DLATGS
Spectral coverage	100–1400 cm^{-1}
Spectral resolution	0.5 cm^{-1}
Optical throughput	0.01 cm^2 sr
Field of view	0.133 rad
Line of sight	nadir, limb, deep space at +30°
Acquisition time	32 s
NESR	0.8–2.5 mW/(m^2 sr cm^{-1})
Mean calibration error	0.1 K

ACPD
7, 17741–17767, 2007

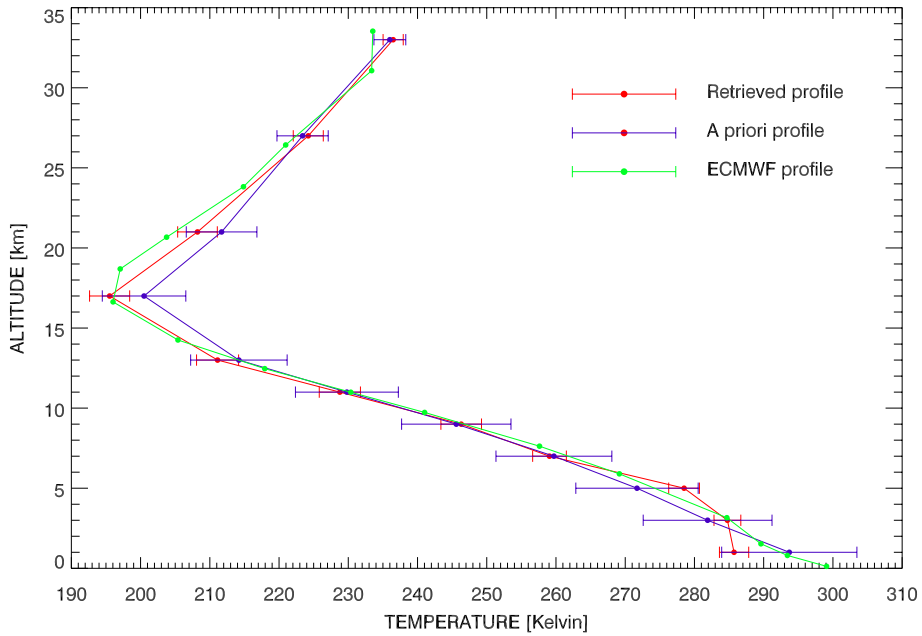

Fig. 1. Retrieval of the T vertical profile (red line) and comparison with the a priori profile (blue line) used as initial guess and with the ECMWF profile (green line).

ACPD
7, 17741–17767, 2007

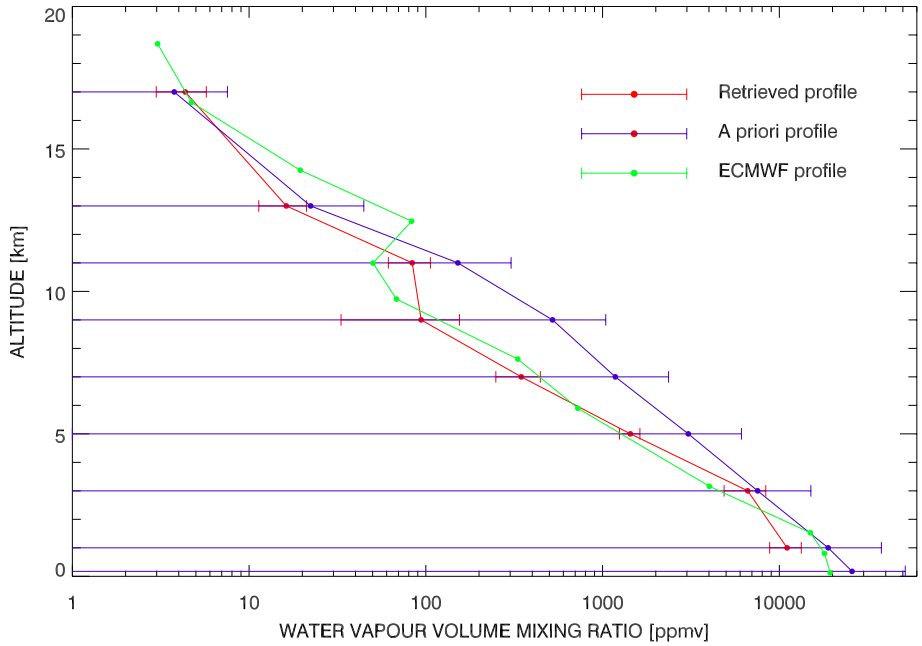

Fig. 2. Retrieval of the water vapour vertical profile (red line) and comparison with the a priori profile (blue line) used as initial guess and with the ECMWF profile (green line).

ACPD
7, 17741–17767, 2007

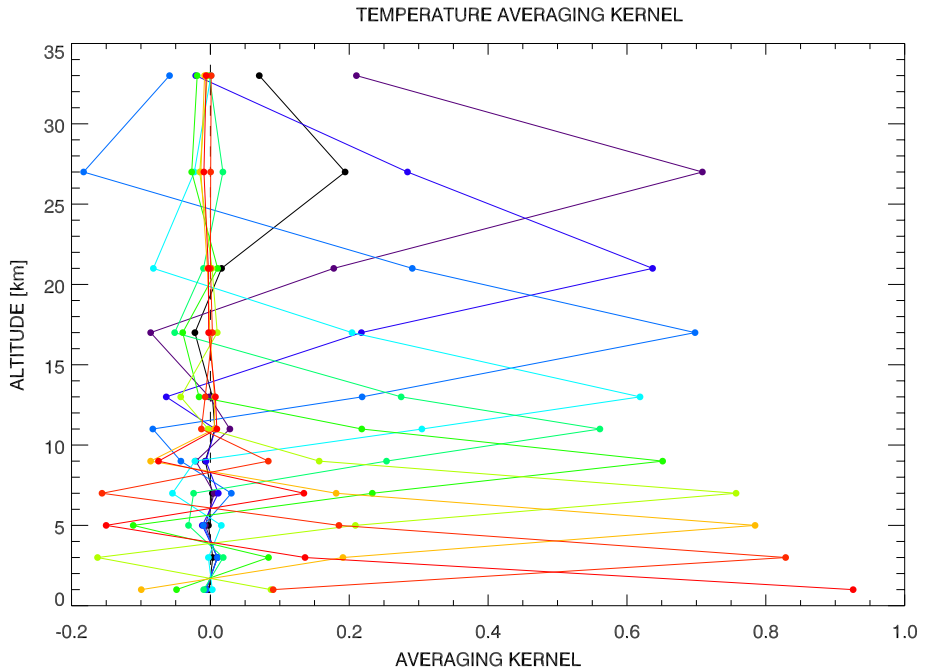

Fig. 3. Averaging kernels for T.

ACPD
7, 17741–17767, 2007

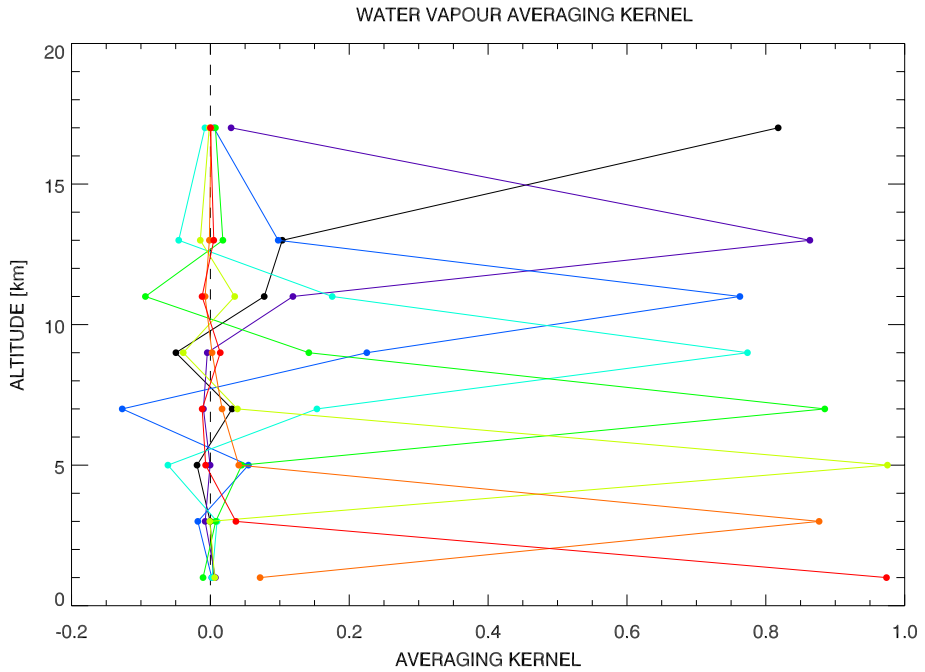

Fig. 4. Averaging kernels for water vapour.

ACPD
7, 17741–17767, 2007

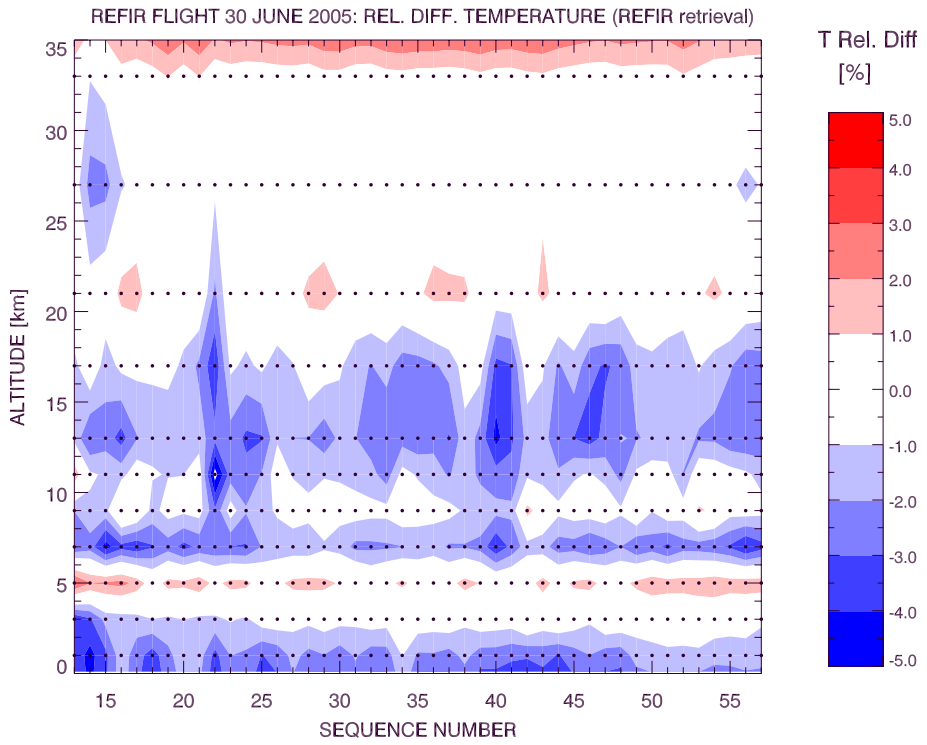

Fig. 5. Difference along the flight between the REFIR retrieved temperature and the ECMWF interpolated fields.

ACPD
7, 17741–17767, 2007

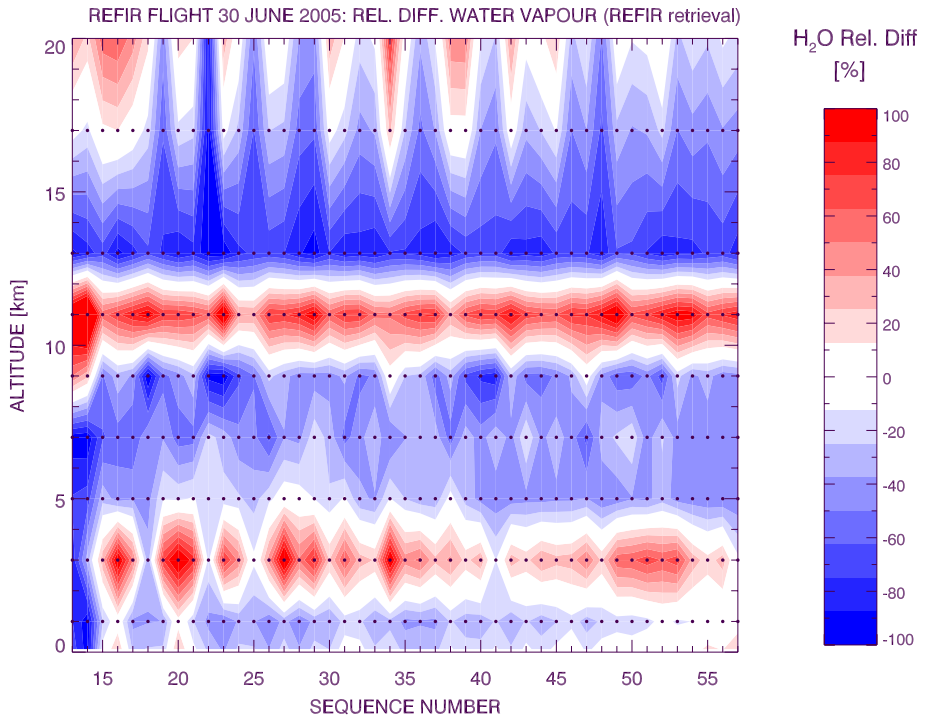

Fig. 6. Difference between water vapour VMR retrieved from the REFIR and the ECMWF interpolated fields.

ACPD
7, 17741–17767, 2007

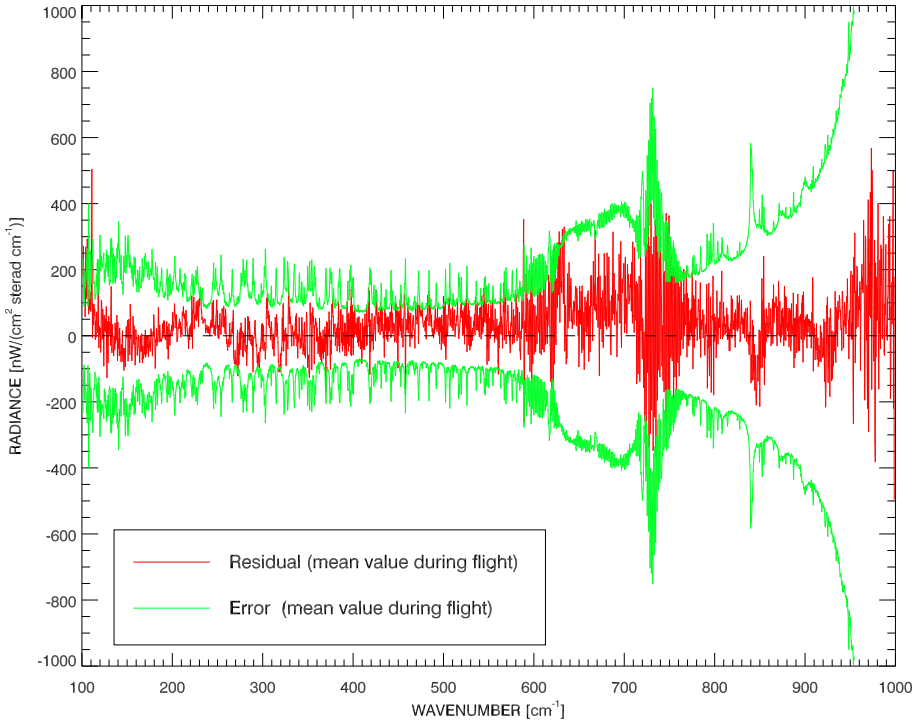

Fig. 7. Mean value of residuals and error during the flight.

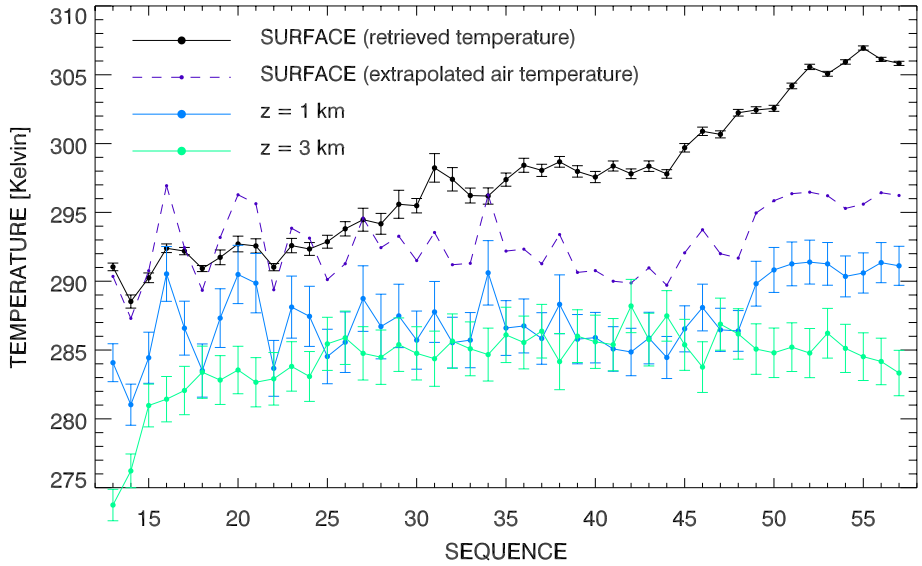

Fig. 8. Time series of temperature values as measured by REFIR at the surface (brightness temperature) and the retrieval altitudes of 1.0 and 3.0 km.

ACPD
7, 17741–17767, 2007

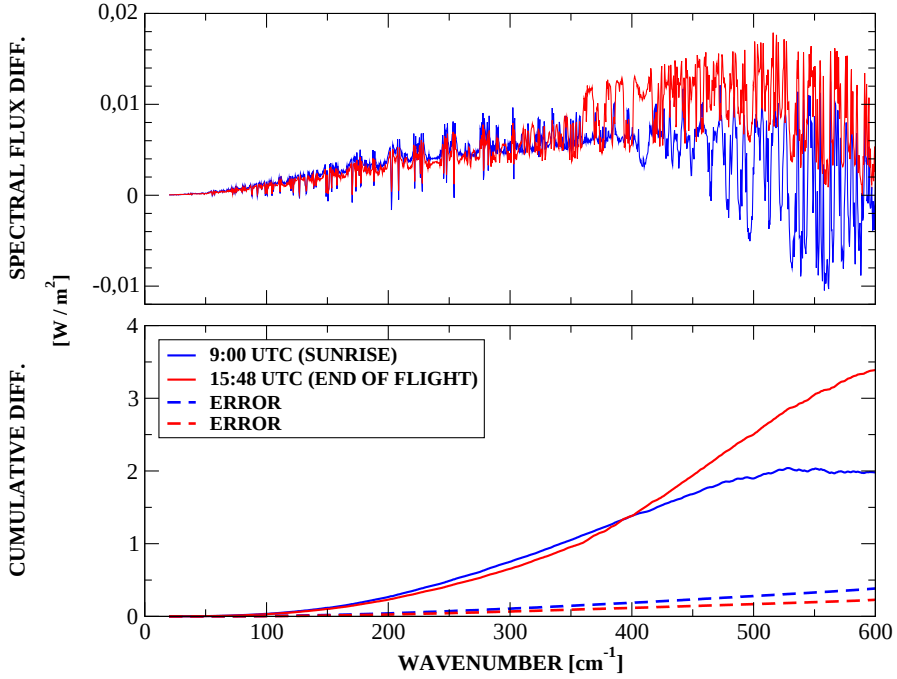

Fig. 9. Difference between the spectral fluxes calculated for the fitted and ECMWF water vapour and temperature profiles. In the figure, the results for 2 sequence measurements are reported as a function of wavenumber (top panel). The cumulative integral is shown in the bottom panel.

ACPD
7, 17741–17767, 2007